

The Conversation: Deep Audio-Visual Speech Enhancement

Triantafyllos Afouras, Joon Son Chung, Andrew Zisserman

Visual Geometry Group, Department of Engineering Science,
University of Oxford, UK

{afourast, joon, az}@robots.ox.ac.uk

Abstract

Our goal is to isolate individual speakers from multi-talker simultaneous speech in videos. Existing works in this area have focussed on trying to separate utterances from known speakers in controlled environments. In this paper, we propose a deep audio-visual speech enhancement network that is able to separate a speaker’s voice given lip regions in the corresponding video, by predicting both the magnitude and the phase of the target signal. The method is applicable to speakers unheard and unseen during training, and for unconstrained environments. We demonstrate strong quantitative and qualitative results, isolating extremely challenging real-world examples.

Index Terms: speech enhancement, speech separation

1. Introduction

In the film *The Conversation* (dir. Francis Ford Coppola, 1974), the protagonist, played by Gene Hackman, goes to inordinate lengths to record a couple’s conversation in a crowded city square. Despite many ingenious placements of microphones, he did not use the lip motion of the speakers to suppress speech from others nearby. In this paper we propose a new model for this task of audio-visual speech enhancement, that he could have used.

More generally, the objective of this paper is to separate the speech signal of a target speaker from background noise and other speakers using visual information from the target speaker’s lips. We propose an audio-visual neural network that can isolate a speaker’s voice from other speakers: given a noisy audio signal and the corresponding speaker video, we produce an enhanced audio signal containing only the target speaker’s voice with the rest of the speakers and background noise suppressed.

Rather than synthesising the voice from scratch, which would be a challenging task, we instead predict a mask that filters the noisy spectrogram of the input. Many speech enhancement approaches focus on refining only the magnitude of the noisy input signal and use the noisy phase for the signal reconstruction. This works well for high signal-to-noise-ratio scenarios, but as the SNR decreases, the noisy phase becomes a bad approximation of the ground truth one [1]. Instead, we propose correction modules for both the magnitude and phase. The architecture is summarised in Figure 1. In training, we initialize the visual stream with a network pre-trained on a word-level lip-reading task, but after this, we train from unlabelled data (Section 3.1) where no explicit annotation is required at the word, character or phoneme-level.

There are many possible applications of this model; one of them is ASR – while machines can recognise speech relatively well in noiseless environments, there is a significant deterioration in performance for recognition in noisy environments [2]. The enhancement method we propose could address this problem, and improve, for example, ASR for mobile phones in

a crowded environment, or automatic captioning for YouTube videos.

The performance of the model is evaluated for up to 5 simultaneous voices, and we demonstrate both strong qualitative and quantitative performance. The trained model is evaluated on unconstrained ‘in the wild’ environments, and for speakers and languages unseen at training time. To the best of our knowledge, we are the first to achieve enhancement under such general conditions. We provide supplementary material with interactive demonstrations on <http://www.robots.ox.ac.uk/~vgg/demo/theconversation>.

1.1. Related works

There are various works that proposed methods to isolate multi-talker simultaneous speech. The majority of these are based on methods that only use the audio, *e.g.* by using voice characteristics of a known speaker [3, 4, 5, 6, 7].

The prevalent method for estimating phase spectra from given magnitudes in speech synthesis is the one proposed by Griffin and Lim [8]. Joint magnitude and phase enhancement has been recently investigated by [9, 10, 1, 11].

A large number of previous works have been developed for audio-visual speech enhancement by predicting masks [12, 13] or otherwise [14, 15, 16, 17, 18, 19, 20, 21]. An overview of

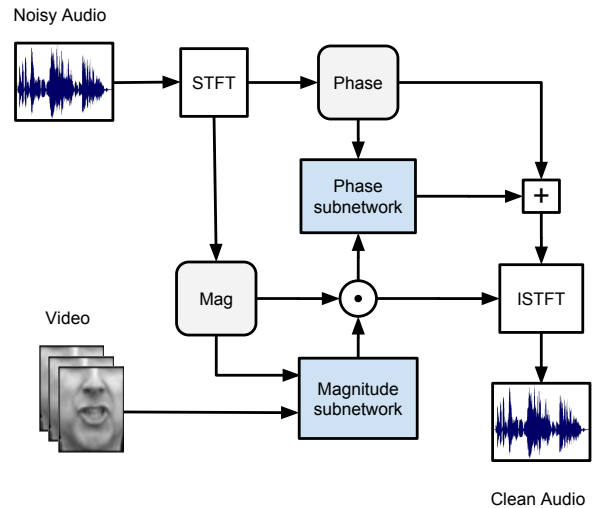


Figure 1: Audio-visual enhancement architecture overview. It consists of two modules: a magnitude sub-network and a phase sub-network. The first sub-network receives the magnitude spectrograms of the noisy signal and the speaker video as inputs and outputs a soft mask. We then multiply the input magnitudes element-wise with the mask to produce a filtered magnitude spectrogram. The magnitude prediction, along with the phase spectrogram obtained from the noisy signal are then fed into the second sub-network, which produces a phase residual. The residual is added to the noisy phase, producing the enhanced phase spectrograms. Finally the enhanced magnitude and phase spectra are transformed back to the time domain, yielding the enhanced signal.

audio-visual source separation is provided by [22]. However, we will concentrate on methods that have built on these using a deep learning framework.

The work of [23] uses a deep neural network model trained to synthesize audio from silent video [24]. The predicted spectrogram is used as a mask to filter the noisy spectrogram. However, the noisy audio signal is not used in the pipeline, and the network is not trained for the task of speech enhancement. In contrast, [25] synthesizes the clean signal conditioning on both the mixed speech input and the input video. The input is passed through an hourglass-like network that processes sets of 5 input frames at a time, along with their corresponding spectrograms. [26] also use a similar audio-visual fusion method, trained to both generate the clean signal and to reconstruct the video. Both papers use the phase of the noisy input signal as an approximation for the clean phase. Although this works for certain scenarios (*e.g.* only one extra speaker), the performance greatly deteriorates as the SNR decreases. Furthermore, these methods are limited in that they are only demonstrated under extremely constrained conditions (*e.g.* the utterances consisting of fixed set of phrases), and for a very small number of speakers that have been seen during training.

Our method differs from these works in a number of ways: (i) It is fully convolutional and therefore applied continuously in time in a sliding-window manner on both the video frames and the spectrograms; (ii) we do not treat the spectrograms as images but as temporal signals with the frequency bins as channels; this allows us to build a deeper network with large number of parameter that trains fast; (iii) we generate a soft mask for filtering instead of directly predicting the clean magnitudes, which we found to be more effective; (iv) we include a phase enhancing sub-network; and, finally, (v) we demonstrate on previously unheard (and unseen) speakers and on in the wild videos.

The enhancement method proposed here is complementary to other examples of audio-visual learning, such as visual speech synthesis [27, 28] and lip reading [29, 30, 31], which has also been shown to improve ASR performance in noisy environments [32, 33].

2. Architecture

This section describes the input representations and architectures for the audio-visual speech enhancement network. The network ingests continuous clips of the audio-visual data. The model architecture is given in detail in Figure 2.

2.1. Video representation

Visual features are extracted from the input image frame sequence with a spatio-temporal residual network similar to the one proposed by [31], pre-trained on a word-level lip reading task. The network consists of a 3D convolution layer, followed by a 18-layer ResNet [34]. For every video frame the network outputs a compact 512 dimensional feature vector f_0^v (where the subscript 0 refers to the layer number in the audio-visual network). Since we train and evaluate on datasets with pre-cropped faces, we do not perform any extra pre-processing, besides conversion to grayscale and an appropriate scaling.

2.2. Audio representation

The acoustic representation is extracted from the raw audio waveforms using Short Time Fourier Transform (STFT) with a Hann window function, which generates magnitude and phase spectrograms. STFT parameters are computed in a similar manner to [25], so that every video frame of the input sequence cor-

responds to four temporal slices of the resulting spectrogram. Since the videos are at 25fps (40ms per frame), we select a hop length of 10ms with a window length of 40ms at a sample rate of 16Khz. The resulting spectrograms have a frequency resolution of 321, representing frequencies from 0 to 8 KHz, and time resolution $T \approx \frac{T_s}{hop}$, where T_s is the number of samples in the signal. The magnitude spectrograms are represented as $T \times 321$ tensors and phase spectrograms as $T \times 642$ tensors, with the real and imaginary components concatenated along the frequency axis.

2.3. Magnitude sub-network

The visual feature sequence f_0^v is processed by a stack of 10 convolutional blocks with kernel width 5 and stride 1. A similar stack of 5 convolutional layers with residual connections is employed for processing the audio stream. The convolutions are performed along the temporal dimension, with the frequencies of the input spectrogram f_0^a viewed as the channels. Two of the intermediate convolutional layers have stride 2, overall down-sampling the temporal dimension by 4, in order to bring it down to the video stream resolution. The skip connections of those layers are down-sampled with average pooling with stride 2. The audio and visual streams are then concatenated over the channel dimension: $f_0^{av} = [f_0^v; f_0^a]$. The fused tensor is passed through another stack of 15 temporal convolution blocks. Since we want the output mask to have the same temporal resolution as the input magnitude spectrogram, two transposed convolutions are used, each up-sampling the temporal dimension by a factor of 2, resulting in a factor of 4 in total. The fusion output is projected through position-wise convolutions onto the input magnitude spectrogram dimensions and passed through a sigmoid activation in order to output a mask with values between 0 and 1. The resulting tensor is multiplied with the noisy magnitude spectrogram element-wise in order to filter it:

$$\hat{M} = \sigma(W_m^T f_{15}^{av}) \odot M_n$$

2.4. Phase sub-network

Our intuition for the phase enhancement sub-network is that there is structure in speech that induces a correlation between the magnitude and phase spectrograms. Similarly to the treatment of the magnitudes, instead of trying to predict the clean phase from scratch, we only predict a residual that refines the noisy phase. The phase sub-network is therefore conditioned on both the noisy phase and the magnitude predictions. These two inputs are fused together after being projecting to 512 dimensions through position-wise convolutions. The fused tensor is then processed by a stack of 6 temporal residual convolution blocks, with 1024 channels each. The phase residual is formed by projecting the result onto the dimensions of the phase spectrogram and is added to the noisy phase. The clean phase prediction is finally obtained by L_2 -normalizing the result:

$$\begin{aligned} \phi_6 &= 6 \times ConvBlock([W_{m\phi}^T \hat{M}; W_{n\phi}^T \Phi_n]) \\ \hat{\Phi} &= \frac{(W_\phi^T \phi_6 + \Phi_n)}{\|(W_\phi^T \phi_6 + \Phi_n)\|_2} \end{aligned}$$

In training, the weights of the layers are initialized with small values and zero biases, so that the initial residuals are nearly zero and the noisy phase is propagated to the output.

2.5. Loss function

The magnitude prediction is obtained by minimizing the L_1 loss between the predicted magnitude spectrogram and the ground

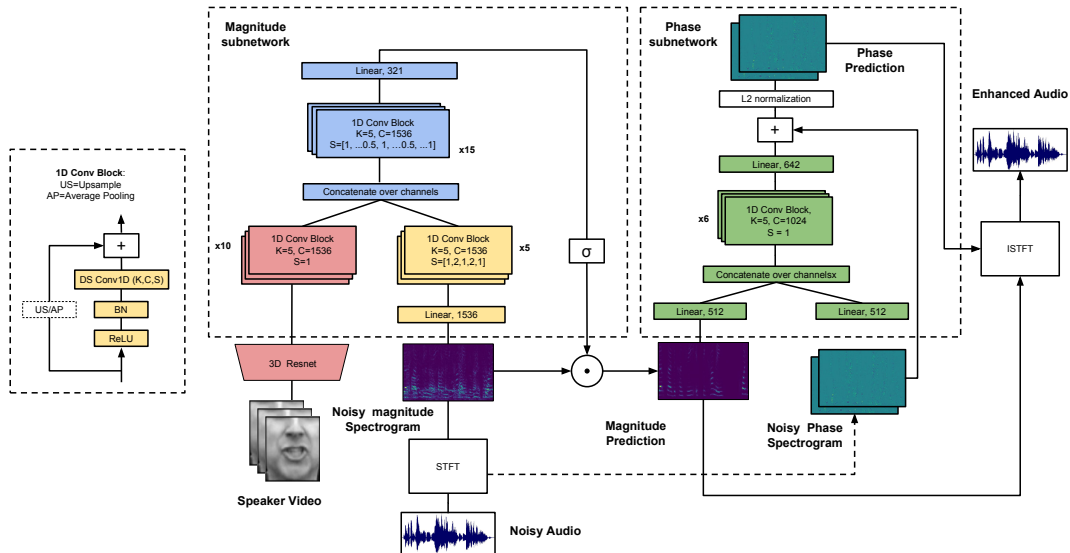


Figure 2: Audio-visual enhancement network. **BN:** Batch Normalization, **C:** number of Channels; **K:** kernel width; **S:** strides – fractional ones denote transposed convolutions. The network consists of a magnitude and a phase sub-network. The basic building unit is a temporal convolutional block with pre-activation [35] shown on the left. Identity skip connections are added after every convolution layer (and speed up training). All convolutional layers have 1536 channels in the magnitude sub-network and 1024 in the phase sub-network. Depth-wise separable convolution layers [36] are used, which consist of a separate convolution along the time dimension for every channel, followed by a position-wise projection on the channel dimensions (equivalent to a convolution with kernel width 1).

truth. The phase prediction is obtained by maximizing the cosine similarity between the phase prediction and ground truth, scaled by the ground truth magnitudes. The overall optimisation objective is $\mathcal{L} = \|\hat{M} - M^*\|_1 - M^* \odot < \hat{\Phi}, \Phi^* >$.

3. Experiments

3.1. Datasets

The model is trained on two datasets: the first is the BBC-Oxford Multi-View Lip Reading Sentences (MV-LRS) dataset [32, 37], which contains thousands of sentences from BBC programs such as Doctors and EastEnders; the second is VoxCeleb2 [38], which contains over a million utterances spoken by over 6,000 different speakers.

The only assumption we make on the datasets is that the audio and video are properly synchronized. Where this is not the case (e.g. TV broadcast), we use the pipeline described in [39] to perform and track active speakers and synchronize the video and the audio.

3.2. Experimental setup

The MV-LRS dataset is divided into training and test sets by broadcast date, in order to ensure that there is no overlapping video between the sets. The dataset covers a large number of speakers, which encourages the trained model to be speaker agnostic. However, since no identity labels are provided with the dataset, there may be some overlapping speakers between the sets. The ground truth transcriptions are provided with the dataset, which allows us to perform quantitative tests on the intelligibility of the generated audio.

The VoxCeleb2 dataset lacks the text transcriptions, however the dataset is divided into training and test sets by identity, which allows us to test the model explicitly for speaker-independent performance.

We examine scenarios where we add 1 to 4 extra interference speakers on the clean signal, therefore we generate signals with 2 to 5 speakers in total. It should be noted that the task of separating the voice of multiple speakers with equal average “loudness” is more challenging than separating the speech signal from ambient background noise.

3.3. Evaluation Protocol

We evaluate the enhancement performance of the model in terms of perceptual speech quality using the blind source separation criteria described in [40]. We use the implementation provided by the PEASS toolkit [41]. The metrics are derived by decomposing the noise present in the enhanced signal into components accounting for different deformations and measuring energy ratios between them. In particular the Signal to Interference Ratio (SIR) measures how well the unwanted signals have been suppressed, the Signal to Artefacts Ratio (SAR) accounts for the introduction of artefacts by the enhancement process, and the Signal to Distortion Ratio (SDR) is an overall quality measure, taking both of the above into account.

Additionally, we use an ASR system to test for the intelligibility of the enhanced speech. For this, we use the Google Speech Recognition interface, and report the Word Error Rates (WER) on the clean, mixed and generated audio samples.

3.4. Training

We pre-train the spatio-temporal visual front-end on a word-level lip reading task, following [31]. Like the authors, we first train on the LRW dataset, consisting of approximately 500K single-word utterances over a vocabulary of 500 words. This dataset covers only near-frontal poses so we further train on an internal multi-view dataset of a similar size. To accelerate the training process, we pre-compute and save the visual features for all the videos in our dataset. We also compute and save the magnitude and phase spectrograms for both the clean and noise audio.

The training takes place in 3 phases: first, we train the magnitude prediction sub-network, following a curriculum which starts with high SNR inputs (i.e. only one additional speaker) and then progressively move to more challenging examples with a greater number of speakers; second, we freeze the magnitude sub-network and train only the phase network; finally, we fine-tune the whole network end-to-end.

To generate training examples we first select a reference pair of visual and audio features (v_r, a_r) by randomly sampling a 60-frame clean segment, making sure that the audio and visual features correspond and are correctly aligned. We then sample

Mag	ϕ	SIR (dB)				SAR (dB)				SDR (dB)				WER (%)			
# Spk.		2	3	4	5	2	3	4	5	2	3	4	5	2	3	4	5
Mix	Mix	—	—	—	—	1.1	-1.6	-3.3	-4.2	-0.3	-3.4	-5.4	-6.7	93.1	99.5	99.9	100
Pr	GT	10.8	13.2	13.8	13.7	21.5	18.3	16.2	14.5	15.7	13.0	10.8	9.5	9.4	12.0	16.7	21.5
Pr	GL	0.9	2.5	3.6	4.0	4.7	4.5	4.3	4.0	-2.9	-2.8	-2.9	-2.7	10.5	13.7	20.3	27.8
Pr	Mix	1.6	2.7	2.5	2.0	17.9	14.6	12.7	11.4	10.5	7.8	5.9	4.8	10.8	14.9	22.0	31.9
Pr	Pr	3.9	5.4	5.4	4.8	18.1	15.1	13.1	11.6	11.8	9.1	7.1	5.8	9.7	13.8	20.3	28.9
GT	GT	Inf.				Inf.				Inf.				8.8			

Table 1: Evaluation of speech enhancement performance on the MV-LRS dataset for scenarios with different number of speakers. The various metrics are listed for the mixed signal and reconstructions using with our model’s predictions. **Mix:** Mixed; **Pr:** Predicted; **GT:** Ground Truth; **GL:** Griffin-Lim; **SIR:** Signal to Interference Ratio; **SAR:** Signal to Artefacts Ratio; **SDR:** Signal to Distortion Ratio (higher is better for all three ratios); **WER:** Word Error Rate (lower is better).

Mag	ϕ	SIR (dB)	SAR (dB)	SDR (dB)
Mix	Mix	-	-1.59	-2.99
Pr	GT	11.05	16.07	11.10
Pr	GL	1.79	3.31	-2.61
Pr	Mix	0.40	13.82	6.71
Pr	Pr	2.32	13.77	7.48

Table 2: Evaluation of speech enhancement performance on the Vox-Celeb2 dataset, for 3 simultaneous speakers, Notations are described in the caption of Table 1.

N noise spectrograms $x_n, n \in [1, N]$, and mix them with the reference spectrogram in the frequency domain by summing up the complex spectra, obtaining the mixed spectrogram a_m . This is a natural way to augment our training data since a different combination of noisy audio signals is sampled every time. Before adding in the noise samples, we normalize their energy to have the reference signal’s one: $a_m = a_r + \sum_n \frac{r_{ms}(x_r)}{r_{ms}(a_n)} a_n$.

3.5. Results

MV-LRS. We summarize our results on the test set of the MV-LRS dataset in Table 1. The performance under the different metrics is listed for the following signal types: The mixed signal which serves as a baseline, and the reconstructions that are obtained using the magnitudes predicted by our network and either the ground truth phase, the phase approximated with the Griffin Lim algorithm, the mixed signal phase or the predicted phase. The signal reconstructed from predicted magnitude and phases is what we consider the final output of our network.

The evaluation when using the ground truth phase is included as an upper bound to the phase prediction. As can be seen by the SAR and SDR of the mixed signal, the task becomes increasingly difficult as more speakers are added. In general the BSS metrics correlate well with our observations. It is interesting to note that while more speakers are added, the SIR stays roughly the same, however more artefacts and overall distortion are introduced. The model is very effective in suppressing cross-talk, and does so with degrading the quality of the output. This can be probably attributed to the masking approach.

The phase predicted by our network performs better than the mixed phase on these criteria. Even though the improvement is relatively small in numbers, the difference in qualitative speech quality is noticeable as the “robotic” effect of having off-synced harmonics is significantly reduced. We encourage the reader to listen to the samples in the supplementary material, where those differences can be understood better. However, the significant gap with the performance of the ground truth phase shows that there is much room for improvement in the phase network.

The transcription results using the Google ASR system are also in line with these findings. In particular, it is noteworthy that our model is able to generate highly intelligible results from noisy audio that is incomprehensible by a human or an ASR system.

Although the content is mainly carried by the magnitude,

we see some major improvement in terms of WER when using a better phase approximation. It is interesting to note that, although the phase obtained using the Griffin Lim (GL) algorithm achieves significantly worse performance on SIR, SAR and SDR, it demonstrates relatively strong WER results, even slightly surpassing the predicted phase by a small margin in the case of 5 simultaneous speakers.

VoxCeleb2. Achieving good enhancement quality on the MV-LRS dataset showcases that our model can generalise across a large number of speakers.

In order to explicitly assess whether our model can generalize to speakers unseen during training, we also train and test on VoxCeleb2, using train, validation and test sets that are disjoint in terms of speaker identities. The results are summarized in Table 2, where we showcase an experiment for the 3-speaker scenario. Overall the performance is comparable to, but slightly worse than, on the MV-LRS dataset – which is in line with the qualitative performance. However, this can be attributed to the visual features not being fine-tuned, and the presence of a lot of other background noise in VoxCeleb2. The results confirm that the method can generalize to unseen (and unheard) speakers.

We should note that even without finetuning on VoxCeleb2 dataset, our original model still works on the dataset, however the performance of the fine-tuned model is better. This is interesting - since the MV-LRS only contains English speakers, but the VoxCeleb2 dataset contains multiple languages, the model learns to generalise to languages not seen during training.

3.6. Discussion

Phase refinement. Estimating the phase from imperfect (predicted) magnitudes is much more challenging compared to estimating from real (ground truth) magnitudes. Our phase enhancement network works very well when trained and evaluated on the ground truth magnitudes, in which case the results are indistinguishable by the human ear. It is much harder to generalize when fed with the imperfect magnitude predictions. Similarly, Griffin Lim also works much better when applied to magnitudes of a real signal.

AV synchronization. Our method is very sensitive to the temporal alignment between the voice and the video. We use SyncNet for the alignment, but since the method can fail under extreme noise, we need to build some invariance in the model. In future work this will be incorporated in the model.

4. Conclusion

In this paper, we have proposed a method to separate the speech signal of a target speaker from background noise and other speakers using visual information from the target speaker’s lips. The deep network produces realistic speech segments by predicting both the phase and the magnitude of the target signal; we have also demonstrated that the network is able to generate intelligible speech from very noisy audio segments recorded in unconstrained ‘in the wild’ environments.

Acknowledgements Funding for this research is provided by the UK EPSRC CDT in Autonomous Intelligent Machines and Systems, the Oxford-Google DeepMind Graduate Scholarship, and by the EPSRC Programme Grant Seebibyte EP/M013774/1.

5. References

- [1] S.-W. Fu, T.-Y. Hu, Y. Tsao, and X. Lu, "Complex spectrogram enhancement by convolutional neural network with multi-metrics learning," *arXiv preprint arXiv:1704.08504*, 2017.
- [2] M. Anusuya and S. K. Katti, "Speech recognition by machine, a review," *arXiv preprint arXiv:1001.2267*, 2010.
- [3] A. M. Reddy and B. Raj, "Soft mask methods for single-channel speaker separation," *IEEE Transactions on Audio, Speech, and Language Processing*, vol. 15, no. 6, pp. 1766–1776, 2007.
- [4] Z. Jin and D. Wang, "A supervised learning approach to monaural segregation of reverberant speech," *IEEE Transactions on Audio, Speech, and Language Processing*, vol. 17, no. 4, pp. 625–638, 2009.
- [5] M. H. Radfar and R. M. Dansereau, "Single-channel speech separation using soft mask filtering," *IEEE Transactions on Audio, Speech, and Language Processing*, vol. 15, no. 8, pp. 2299–2310, 2007.
- [6] S. Makino, T.-W. Lee, and H. Sawada, *Blind speech separation*. Springer, 2007, vol. 615.
- [7] D. Wang and J. Chen, "Supervised speech separation based on deep learning: an overview," *arXiv preprint arXiv:1708.07524*, 2017.
- [8] D. Griffin and J. S. Lim, "Signal estimation from modified short-time fourier transform," *Acoustics, Speech and Signal Processing, IEEE Transactions on*, vol. 32, pp. 236 – 243, 05 1984.
- [9] D. S. Williamson, Y. Wang, and D. Wang, "Complex ratio masking for joint enhancement of magnitude and phase," in *Proc. ICASSP*, 03 2016, pp. 5220–5224.
- [10] H.-G. Hirsch and M. Gref, "On the influence of modifying magnitude and phase spectrum to enhance noisy speech signals," in *Interspeech*, 08 2017, pp. 1978–1982.
- [11] M. L. Dubey, G. T. Kenyon, N. Carlson, and A. Thresher, "Does phase matter for monaural source separation?" *CoRR*, vol. abs/1711.00913, 2017.
- [12] Q. Liu, W. Wang, P. J. Jackson, M. Barnard, J. Kittler, and J. Chambers, "Source separation of convolutive and noisy mixtures using audio-visual dictionary learning and probabilistic time-frequency masking," *IEEE Transactions on Signal Processing*, vol. 61, no. 22, pp. 5520–5535, 2013.
- [13] F. Khan and B. Milner, "Speaker separation using visually-derived binary masks," in *Auditory-Visual Speech Processing (AVSP) 2013*, 2013.
- [14] W. Wang, D. Cosker, Y. Hicks, S. Saneit, and J. Chambers, "Video assisted speech source separation," in *Proc. ICASSP*, vol. 5. IEEE, 2005, pp. v–425.
- [15] L. Girin, J.-L. Schwartz, and G. Feng, "Audio-visual enhancement of speech in noise," *The Journal of the Acoustical Society of America*, vol. 109, no. 6, pp. 3007–3020, 2001.
- [16] S. Deligne, G. Potamianos, and C. Neti, "Audio-visual speech enhancement with avcdcn (audio-visual codebook dependent cepstral normalization)," in *Sensor Array and Multichannel Signal Processing Workshop Proceedings, 2002*. IEEE, 2002, pp. 68–71.
- [17] J. R. Hershey and M. Casey, "Audio-visual sound separation via hidden markov models," in *NIPS*, 2002, pp. 1173–1180.
- [18] J. Hershey, H. Attias, N. Jovic, and T. Kristjansson, "Audio-visual graphical models for speech processing," in *Proc. ICASSP*, vol. 5. IEEE, 2004, pp. V–649.
- [19] I. Almajai and B. Milner, "Using audio-visual features for robust voice activity detection in clean and noisy speech," in *Signal Processing Conference, 2008 16th European*. IEEE, 2008, pp. 1–5.
- [20] I. Almajai and B. P. Milner, "Effective visually-derived wiener filtering for audio-visual speech processing," in *AVSP*, 2009.
- [21] R. Goecke, G. Potamianos, and C. Neti, "Noisy audio feature enhancement using audio-visual speech data," in *Proc. ICASSP*, vol. 2, May 2002, pp. II–2025–II–2028.
- [22] S. M. N. BertrandRivet, WenwuWang and J. A. Chambers, "Audiovisual speech source separation: An overview of key methodologies," *IEEE Signal Processing Magazine*, vol. 31, 2014.
- [23] A. Gabbay, A. Ephrat, T. Halperin, and S. Peleg, "Seeing through noise: Visually driven speaker separation and enhancement," *arXiv preprint arXiv:1708.06767*, 2017.
- [24] A. Ephrat, T. Halperin, and S. Peleg, "Improved speech reconstruction from silent video," in *ICCV 2017 Workshop on Computer Vision for Audio-Visual Media*, 2017.
- [25] A. Gabbay, A. Shamir, and S. Peleg, "Visual Speech Enhancement using Noise-Invariant Training," *arXiv preprint arXiv:1711.08789*, 2017.
- [26] J.-C. Hou, S.-S. Wang, Y.-H. Lai, Y. Tsao, H.-W. Chang, and H.-M. Wang, "Audio-Visual Speech Enhancement based on Multimodal Deep Convolutional Neural Networks," *arXiv preprint arXiv:1703.10893*, 2017. [Online]. Available: <http://arxiv.org/abs/1703.10893>
- [27] S. Suwajanakorn, S. M. Seitz, and I. Kemelmacher-Shlizerman, "Synthesizing obama: learning lip sync from audio," *ACM Transactions on Graphics (TOG)*, vol. 36, no. 4, p. 95, 2017.
- [28] J. S. Chung, A. Jamaludin, and A. Zisserman, "You said that?" in *Proc. BMVC.*, 2017.
- [29] J. S. Chung and A. Zisserman, "Lip reading in the wild," in *Proc. ACCV*, 2016.
- [30] Y. M. Assael, B. Shillingford, S. Whiteson, and N. de Freitas, "Lipnet: Sentence-level lipreading," *arXiv:1611.01599*, 2016.
- [31] T. Stafylakis and G. Tzimiropoulos, "Combining residual networks with lstms for lipreading," in *Interspeech*, 2017.
- [32] J. S. Chung, A. Senior, O. Vinyals, and A. Zisserman, "Lip reading sentences in the wild," in *Proc. CVPR*, 2017.
- [33] S. Petridis, T. Stafylakis, P. Ma, F. Cai, G. Tzimiropoulos, and M. Pantic, "End-to-end audiovisual speech recognition," *CoRR*, vol. abs/1802.06424, 2018.
- [34] K. He, X. Zhang, S. Ren, and J. Sun, "Deep residual learning for image recognition," *arXiv preprint arXiv:1512.03385*, 2015.
- [35] K. He, X. Zhang, S. Ren, and J. Sun, "Identity mappings in deep residual networks," in *Proc. ECCV*, 2016, pp. 630–645.
- [36] F. Chollet, "Xception: Deep learning with depthwise separable convolutions," in *Proc. CVPR*, 2017, pp. 1251–1258.
- [37] J. S. Chung and A. Zisserman, "Lip reading in profile," in *Proc. BMVC.*, 2017.
- [38] J. S. Chung, A. Nagrani, , and A. Zisserman, "Voxceleb2: Deep speaker recognition," in *arXiv*, 2018.
- [39] J. S. Chung and A. Zisserman, "Out of time: automated lip sync in the wild," in *Workshop on Multi-view Lip-reading, ACCV*, 2016.
- [40] R. G. C. Fevotte and E. Vincent, "Bss eval toolbox user guide," *IRISA Technical Report 1706, Rennes, France, April 2005*. http://www.irisa.fr/metiss/bss_eval/, 2005.
- [41] N. H. Valentin Emiya, Emmanuel Vincent and V. Hohmann, "Subjective and objective quality assessment of audio source separation," *IEEE Transactions on Audio, Speech and Language Processing*, pp. 2046–2057, 2011.